

# SIMULATION OF DOUBLE BASE PROPELLANT COMBUSTION USING THE ICT-CELLULAR-COMBUSTION-ALGORITHM

**Sebastian Wurster**

Fraunhofer Institute for Chemical Technology, Joseph-von-Fraunhoferstr. 7, D-76327  
Pfinztal-Berghausen, Germany

Corresponding Author: [sebastian.wurster@ict.fraunhofer.de](mailto:sebastian.wurster@ict.fraunhofer.de)

## **Abstract**

Closed vessel experiments with a 7 perforated double base propellant have been conducted and are compared to simulation results from a new interior ballistic model. The new model implements the two dimensional ICT-Cellular-Combustion-Algorithm (ICCA) which makes it possible to simulate 2D form functions of propellant cross sections. Together with a preprocessing algorithm and a lumped parameter model based on STANAG 4367 this makes the simulation of 3D propellants with a complex cross sectional geometry possible. The used lumped parameter model goes beyond STANAG 4367 in considering the pressure dependent thermochemistry of the product gases. It is shown that the new model is able to reproduce the dynamic vivacities from closed vessel experiments with a high degree of accuracy.

**Keywords:** ICCA2D, ICT-Cellular-Combustion-Algorithm, Propellant, Combustion, Modeling, Interior Ballistics, Energetic Materials, Closed Vessel, Form Function, Thermochemistry

## **Introduction**

Key to every simulation of solid propellant burning is the knowledge of the gas production rate  $dz/dt$  where  $z$  is the burned mass fraction of the propellant. It can be written as in eq. 1.

$$\frac{dz}{dt} = \left(\frac{S_0}{V_0}\right) \cdot \left(\frac{S}{S_0}\right) \cdot r(p) = \left(\frac{S_0}{V_0}\right) \cdot \varphi(z) \cdot \beta \left(\frac{p}{p_0}\right)^\alpha \quad (1)$$

Here  $S_0$  and  $V_0$  are the surface and volume of the unburned propellant grain, the form function  $\varphi(z)$  is the ratio of the burning surface  $S$  to the initial surface  $S_0$  and  $r(p)$  is the pressure

dependent linear burning velocity which is most often described by Vieille's law with the normal pressure burning velocity  $\beta$  and pressure exponent  $\alpha$ . Together with an appropriate equation of state and suitable boundary conditions this is sufficient to simulate the combustion process. The thermodynamic properties of the product gases can be calculated, e.g. with the ICT-Thermodynamic-Code [1][2]. The parameters  $\alpha$  and  $\beta$  cannot readily be calculated from first principles but are deduced from pressure time curves or by visual observation of strand burning.

The form function, initial surface and initial volume have to be calculated from the geometry of the unburned propellant grains and the form function has to be known as an analytical function which is only possible for highly symmetrical propellant grain shapes, e.g. cylindrical, 1 perforated, 7 perforated or 19 perforated grains. To go beyond the boundaries of the traditional form function formalism the so called ICT-Cellular-Combustion-Algorithm (ICCA) was developed at the Fraunhofer ICT in recent years [3][4][5]. ICCA is based on cellular automata and describes the propellant geometry as an array of cells which evolve during the combustion process according to simple rules, see Figure 1. The burned mass fraction and form function is then extracted from the array during every computational step.

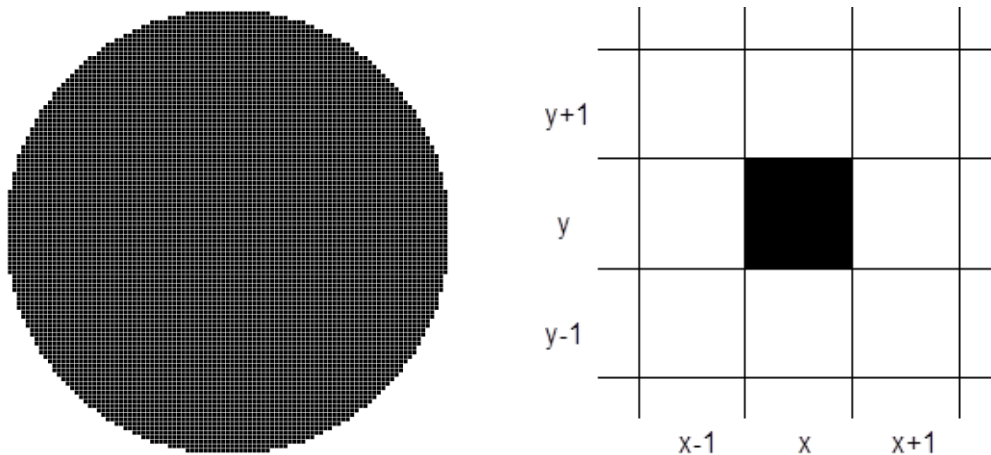


Figure 1: Propellant grain cross section as a composition of individual cells in ICCA2D, black color indicates propellant filled cells

In this work first the theoretical model is presented. Next the results from closed vessel experiments with the 7 perforated double base propellant JA2 are compared to simulation results using the new model. It is shown that the new model is able to reproduce the dynamic vivacities from closed vessel experiments with a high degree of accuracy.

## Theoretical Model

Details of the basic model are published elsewhere so the reader is referred to the literature for in depth information [4][5]. Only the basic features are presented here. The model uses black and white bitmaps of the propellant geometry as input data. In a first preprocessing step the area  $A_0$  and circumference  $U_0$  of the 2D geometry are determined. After that the ICCA2D is used to simulate the 2D form function  $\varphi^{2D}(z^{2D})$  of the cross section which is available in tabular form at the end of the calculation. The calculated 2D parameters can be linked to the needed 3D parameters by eq. 2 – 4. via the initial grain length  $l_0$  and the current grain length  $l$ . This makes the simulation of extrudable propellant grain geometries possible.

$$z^{2D} := 1 - \frac{A}{A_0} \quad \varphi^{2D} := \frac{U}{U_0} \quad (2)$$

$$z^{3D} = 1 - \frac{A \cdot l}{A_0 \cdot l_0} = 1 - (1 - z^{2D}) \frac{l}{l_0} \quad (3)$$

$$\varphi^{3D} = \frac{U \cdot l + 2 \cdot A}{U_0 \cdot l_0 + 2A_0} = \frac{U_0 \cdot \varphi(z^{2D}) \cdot l + 2 \cdot A_0 \cdot (1 - z^{2D})}{U \cdot l_0 + 2 \cdot A_0} \quad (4)$$

After the 2D simulations with ICCA are finished the simulation of the 3D combustion process can proceed. For this the lumped parameter model from STANAG 4367 [6] has been adapted and expanded to account for pressure dependent thermochemistry. In the timestep (i+1) the burned mass fraction  $z_{i+1}^{3D}$  and propellant length are calculated first according to

$$z_{t+1}^{3D} = \frac{S_0}{V_0} \cdot \varphi(z_i^{3D}) \cdot r(p_i) \cdot \delta t + z_i^{3D} \quad l_{t+1} = l_t - 2 \cdot r_t(p) \cdot \delta t \quad (5)$$

Here  $\delta t$  is the timestep width and the index  $t$  denotes the computational step. Note that the 3D form function is not yet known in the current timestep but in the step  $i=1$  the calculation of the burned mass fraction is possible because by definition  $\varphi^{3D}(0) = 1$ . Next the new pressure can be calculated according to the STANAG model, see eq. 6-8.

$$p_{t+1} = \frac{T_{t+1}}{V_{t+1}} \left( \frac{F(p) \cdot C \cdot z_{t+1}^{3D}}{T^{ad}(p)} + \frac{F_I \cdot C_I}{T_I^{ad}} \right) \quad (6)$$

$$T_{t+1} = \frac{\frac{F(p) \cdot C \cdot z_{t+1}^{3D}}{\kappa(p) - 1} + \frac{F_I \cdot C_I}{\kappa_I - 1} - E_t^h}{\frac{F(p) \cdot C \cdot z_{t+1}^{3D}}{(\kappa(p) - 1) \cdot T^{ad}(p)} + \frac{F_I \cdot C_I}{(\kappa_I - 1) \cdot T_I^{ad}}} \quad (7)$$

$$V_{t+1} = V_0 - \frac{C}{\rho} \cdot (1 - z_{t+1}^{3D}) - C \cdot \eta(p) \cdot z_{t+1}^{3D} - C_I \cdot \eta_I \quad (8)$$

Here all variables with an index I belong to the igniter which is not modelled in detail but is assumed to have been converted entirely to gas at the beginning of the simulation so it only provides a starting pressure for the combustion of the propellant.  $p_{t+1}$  is the pressure,  $T_{t+1}$  is the mixing temperature of propellant and igniter gas,  $C$  and  $\rho$  are the propellant mass and density,  $V_0$  is the volume of the closed vessel and  $V_{t+1}$  is the free volume which is corrected for the remaining propellant volume and covolumes of the igniter and propellant gases. Note that in addition to the STANAG the thermodynamical variables force  $F$ , adiabatic flame temperature  $T^{ad}$ , ratio of specific heats  $\kappa$  and covolume  $\eta$  are considered pressure dependent. Heat loss by conduction to the walls is considered by the factor  $E_t^h$  which is calculated according to STANAG 4367 [6].

At last the 3D form function for the next timestep is computed by using eq. 3 to determine  $z_{i+1}^{2D}$ , then interpolate on the ICCA results to get  $\varphi^{2D}(z_{i+1}^{2D})$  and finally use eq. 4 to calculate  $\varphi^{3D}(z_i^{3D})$ .

After completion of the simulation the dynamic vivacity is calculated according to eq. 9.

$$L(p_t/p_{max}) = \frac{p_{t+1} - p_t}{\delta t \cdot p_t \cdot p_{max}} \quad (9)$$

## Simulation of Experimental Results

Closed vessel tests with the double base propellant JA2 have been conducted at loading densities of 0.1 g/cm<sup>3</sup>, 0.15 g/cm<sup>3</sup>, 0.2 g/cm<sup>3</sup> and 0.25 g/cm<sup>3</sup> with three shots at each loading density. JA2 was chosen because it has been widely studied and a lot of information is available in the literature. The composition and thermodynamic data for example can be found in [7] and [8]. The burning behavior has also been extensively studied and numerous information on burn rates of JA2 can be found in the literature [9][10][11][12]. Juhasz et.al. for example give a burn rate exponent of  $\alpha = 0.9517$  and  $\beta = 0.1313$  mm/s for measurements in a 200 cm<sup>3</sup> closed vessel at a loading density of 0.34 g/cm<sup>3</sup> [13].

The closed vessel that was used has a volume of 306 cm<sup>3</sup> and was equipped with a Kistler 6215 pressure transducer. The ignition consisted of a Sobbe SO7 igniter together with 1g of B/KNO<sub>3</sub>. From the closed vessel data the dynamic vivacities were calculated and a single set of Vieille's parameters can be determined as described in the literature [14][15]. The parameters  $\alpha$  and  $\beta$  have been averaged to match the results from all loading densities as good as possible with only one set of parameters. For all simulations  $\alpha = 0.9544$  and  $\beta = 0.1438$  mm/s were used.

To get the geometric input data for the simulation computer tomographic cross sections of the propellant grains were produced in a Mikro-CT model 1076 by Skyscan. Its maximum power is 10 W and the maximum voltage is 100 kV. The maximal resolution is 9  $\mu\text{m}$  / pixel. The resolution of the computer tomographic images was chosen to be 18.64  $\mu\text{m}$  / pixel. The images were then binarized so that they can be used as input for the model. The processed image used in the simulations is shown in Figure 2. The length of the propellant grains was also measured and a value of 13.93 mm was chosen for the simulations.

The thermodynamic variables were calculated with the ICT-Thermodynamic-Code for isochoric conditions with different fixed end pressures with the composition given by Conner et.al. [8]. The results of these calculations can be seen in Figure 3. As shown the force  $F$ , adiabatic flame temperature  $T$  and ratio of specific heats  $\kappa$  are getting bigger while the covolume  $\eta$  is getting smaller with increasing pressure. This reflects the shifting of the chemical equilibria with increasing pressure.

Finally the numerical implementation of the model uses a finite difference scheme to integrate eq. 5. The pressure dependent thermodynamic data is interpolated using a cubic spline to avoid oscillations during the calculation of the dynamic vivacity. Where no data is available extrapolation is used. First the pressure vs. time curve is simulated and in a second step the dynamic vivacity is calculated according to eq. 9.

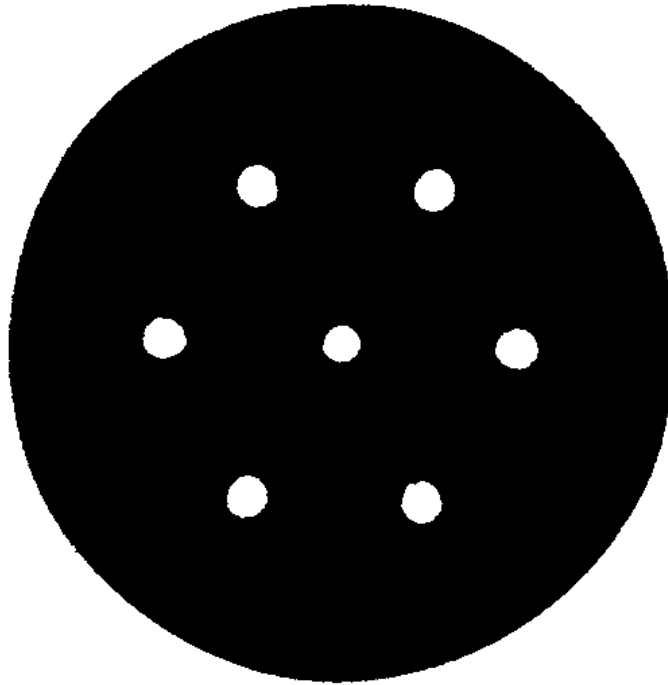


Figure 2: Processed computer tomographic cross section of JA2 grain used as input data for simulations

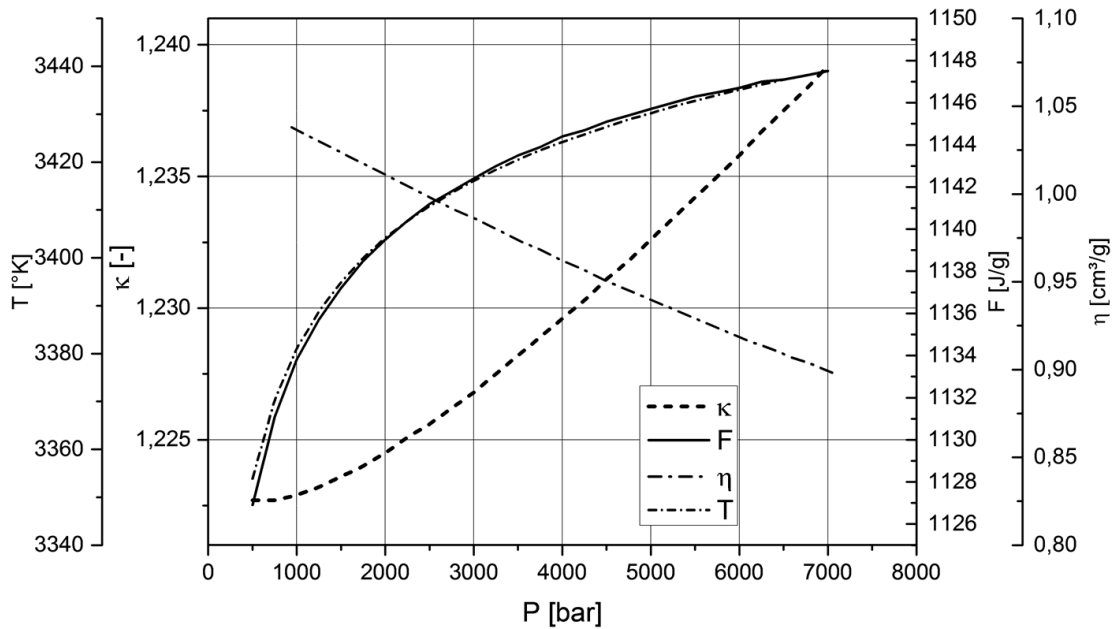


Figure 3: Pressure dependence of thermodynamic parameters in the range between 500 and 7000 bar for constant volume calculated with the ICT-Thermodynamic-Code

The results of the simulations and the comparison to the experimental vivacities are shown in Figure 4, Figure 5, Figure 6 and Figure 7. The experimental vivacities are labelled with increasing numbers from V013 to V024. The dynamic vivacities for each loading density agree well with the largest variations present at 0.1 g/cm<sup>3</sup>. The overall agreement between the simulations and the experimental results is also quite good. Deviations can be seen in the beginning up to  $p/p_{max}$  values of 0.3 and after the slivering point from 0.75 to 1 for all loading densities. The deviations in the beginning are due to non-ideal ignition behavior of the propellant grains. Not all grains are ignited at the same time and on the entire surface. As can be seen this gets less and less pronounced as the loading density is increased. Also the slivering is more smeared out since not all propellant grains reach the slivering point at the same  $p/p_{max}$  value. Such deviations are for example caused by small geometry variations in between the propellant grains. Although complex propellant cross sections can be simulated the model still assumes that all grains are uniform in shape and burn alike. The main part of the burning between  $p/p_{max}$  values of 0.3 and 0.75 on the other hand is captured very well by the simulations with the biggest deviations present for a loading density of 0.1 g/cm<sup>3</sup>.

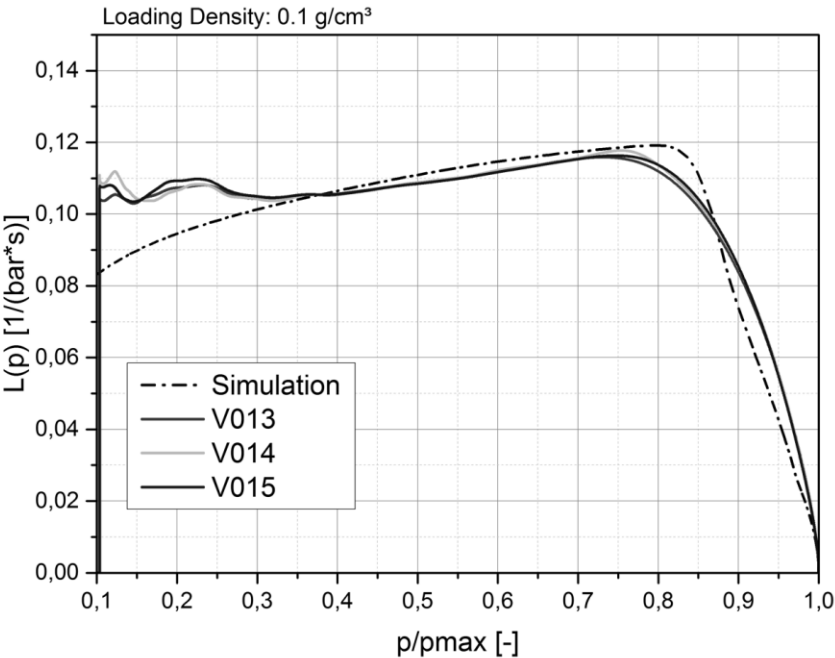


Figure 4: Comparison of experimental and simulated dynamic vivacities at 0.1 g/cm<sup>3</sup> loading density

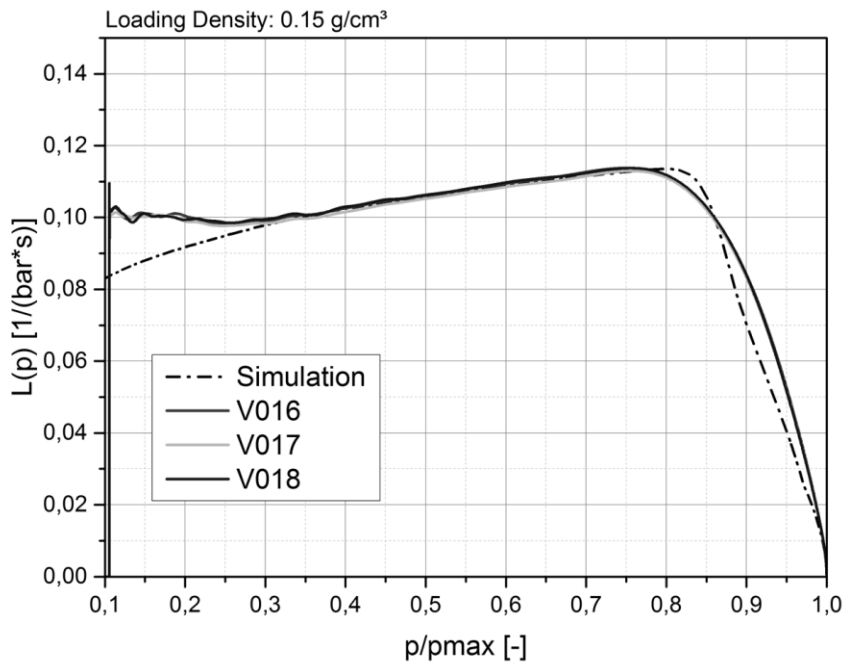


Figure 5: Comparison of experimental and simulated dynamic vivacities at 0.15 g/cm<sup>3</sup> loading density

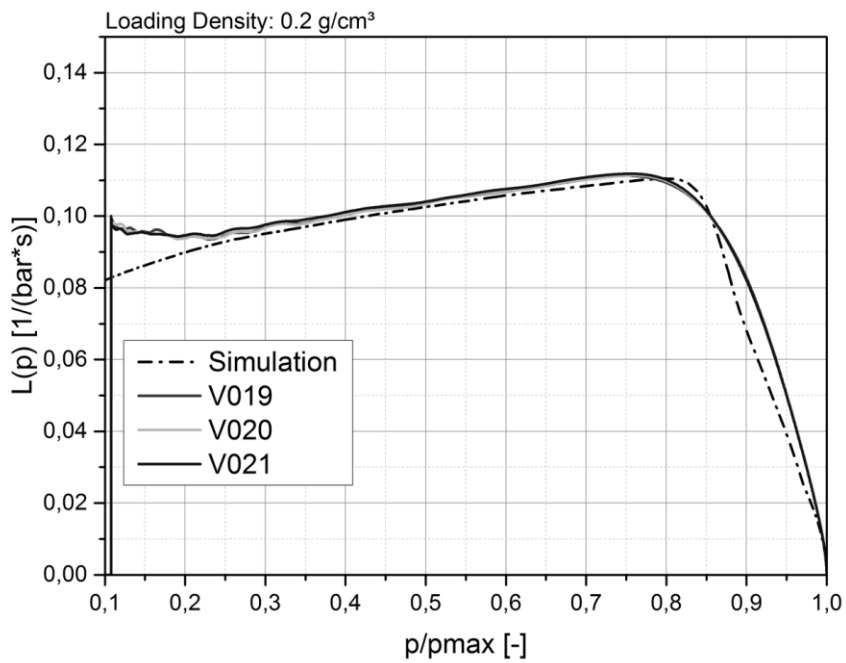


Figure 6: Comparison of experimental and simulated dynamic vivacities at 0.2 g/cm<sup>3</sup> loading density

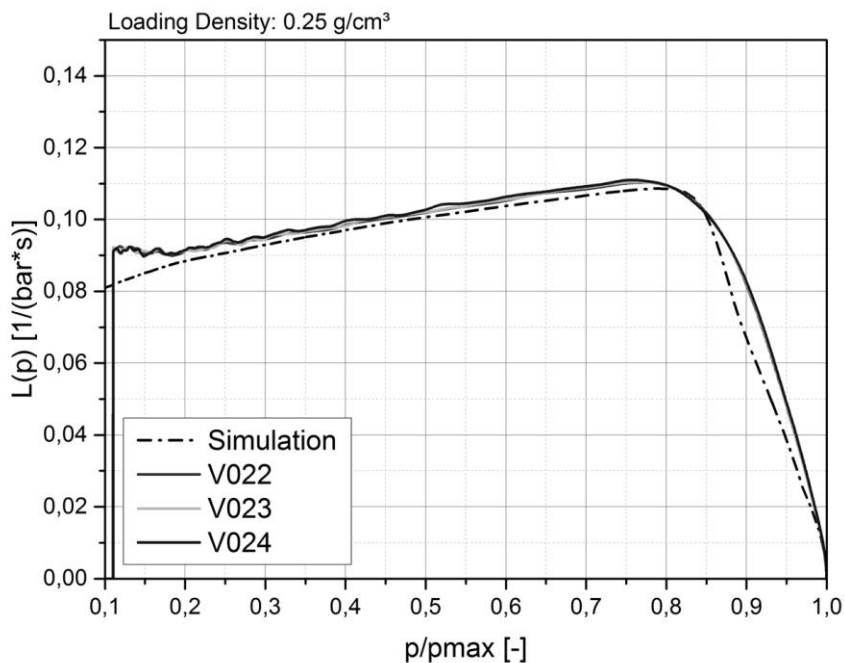


Figure 7: Comparison of experimental and simulated dynamic vivacities at 0.25 g/cm<sup>3</sup> loading density

## Summary

A new model to simulate the combustion behavior of propellants with complex cross sectional geometry has been presented. It incorporates the 2D ICT-Cellular-Combustion-Algorithm which numerically simulates the 2D form function of a propellant cross section. Together with preprocessing algorithms and a STANAG 4367 based lumped parameter model which takes into account the pressure dependence of the thermodynamic parameters this makes the simulation of 3D propellants with arbitrary cross sectional geometry possible.

Processed computer tomographic cross sections of real propellant grains are used as geometric input for the model. The thermodynamic parameters and their pressure dependence are calculated with the ICT-Thermodynamic-Code. Vieille's parameters  $\alpha$  and  $\beta$  are deduced from the experimental pressure vs. time curves. Experimental results from closed vessel tests for the double base propellant JA2 at different loading densities are presented and compared to simulation results. The comparison between experimental and simulated dynamic vivacities shows good agreement. Deviations during ignition and slivering can be seen which are due to variations from grain to grain not explicitly captured in the model. Although complex propellant cross sections can be simulated it still assumes that all grains are uniform in shape and combustion behavior. This could be overcome in the future by simulating the combustion of every propellant grain in the closed vessel with the presented model.

## Acknowledgments

This work is supported by the Bundeswehr Technical Center for Weapons and Ammunition (WTD 91) in Meppen.

## References

- [1] Volk, F.; Bathelt, H.; User's Manual for the ICT-Thermodynamic Code; Vol. 2; Proceedings of the 27th International Annual Conference of ICT, Karlsruhe, Germany, 92/1-16, 1996
- [2] Kempa, P.B.; Bathelt, H.; Volk, F.; Weindel, M.; "ICT-Database of Thermochemical Values, Eighth Update (2008)"
- [3] Fischer, T.S.; Messmer, A.; Burning Characteristics of Foamed Polymer Bonded Propellants; Proceedings of the 19<sup>th</sup> International Symposium on Ballistics, Interlaken, Switzerland, 2001
- [4] Wurster, S.; Fischer, T.S.; Simulation of Propellant Combustion Using the ICT-Cellular-Combustion-Algorithm (ICCA); Proceedings of the 28th International Symposium on Ballistics, Atlanta, USA, 2014
- [5] Wurster, S.; Fischer, T.S.; Simulation of Closed Vessel Combustion Using the 2D ICT-Cellular-Combustion-Algorithm; Proceedings of the 29th International Symposium on Ballistics, Edinburgh, UK, 2016
- [6] STANAG 4367 (Edition 3) - Thermodynamic Interior Ballistic Model with Global Parameters; NATO Standardization Agency, 2009
- [7] Lieb, R.J.; The Mechanical Response of M30, JA2 and XM39 Gun Propellants to High Rate Deformation, ADA213328, ARMY BALLISTIC RESEARCH LAB ABERDEEN PROVING GROUND MD, August 1989
- [8] Conner, Clint B.; Anderson, William R. (2009): Modeling the combustion of JA2 and solid propellants of similar composition. In: Proceedings of the Combustion Institute 32 (2), S. 2131–2137. DOI: 10.1016/j.proci.2008.06.059.
- [9] Miller, M.S.; Anderson, W.R.; CYCLOPS – a Breakthrough Code to predict Solid-Propellant Burning Rates; U.S. Army Research Laboratory Technical Report; ARL-TR-2910, February 2003
- [10] Kuo, Kenneth K.; Zhang, Baoqi (2006): Transient Burning Characteristics of JA2 Propellant Using Experimentally Determined Zel'dovich Map. In: Journal of Propulsion and Power 22 (2), S. 455–461. DOI: 10.2514/1.4871.

- [11] Weiser, V.; Kelzenberg, S.; Fischer, T.; Baier, A.; Langer, G.; Eisenreich, N.; Eckl, W.; Burning Phenomena of Doublebase Gun Propellant JA2. In: Propellants, Explosives and Pyrotechnics (25), S. 143–148., 2000
- [12] Horst, A.W.; Baker, P.J.; Rice, B.M.; Kaste, P.J.; Colburn, J.W.; Hare, J.J.; Insensitive High Energy Propellants for Advanced Gun Concepts; U.S. Army Research Laboratory Technical Report; ARL-TR-2584, October 2001
- [13] Juhasz, A.A.; Bullock, C.D.; Homan, B.; Devynck, D.; Micro Closed Bomb for Characterizing the Burning of Propellants at Gun Pressures; Proceedings of the 36<sup>th</sup> JANNAF Combustion Subcommittee, 1999
- [14] STANAG 4115 LAND (Edition 2) – Definition and Determination of Ballistic Properties of Gun Propellants; NATO Standardization Agency, 1997
- [15] Hund, M.; Eisenreich, N.; Volk, F.; Determination of Interior Ballistic Parameters of Solid Propellants by Different Methods; Proceedings of the 6<sup>th</sup> International Symposium on Ballistics, Orlando, USA, 1981